FACTA UNIVERSITATIS
Series: **Electronics and Energetics** Vol. 37, Nº 3, September 2024, pp. 423 – 435
https://doi.org/10.2298/FUEE2403423K

Original scientific paper

ANALYSIS OF FOUR CIRCULAR COIL CONFIGURATION FOR UNIFORMLY DISTRIBUTED MAGNETIC FIELD GENERATION*

Karolina Kasaš-Lažetić, Miodrag Milutinov, Teodora Spasić, Gorana Mijatović

University of Novi Sad, Faculty of Technical Sciences

ORCID iDs:	Karolina Kasaš-Lažetić	https://orcid.org/0000-0003-1502-450X
	Miodrag Milutinov	https://orcid.org/0000-0002-1725-3405
	Teodora Spasić	https://orcid.org/0000-0002-5490-1045
	Gorana Mijatović	https://orcid.org/0000-0002-7409-8130

Abstract. *A uniform magnetic field can be achieved with various simple structures of circular or square cross-sections. The main purpose of each of these is to create a larger volume of uniformly distributed magnetic field. The improvement of the desired zone homogeneity can be achieved by varying the design parameters of the coil and applying different optimization algorithms. In this paper, the Lee-Whiting circular coil system has been investigated considering the cross-section of the real conductor instead of the volumeless ideal conductor. The parameters of the coil were optimized to achieve a uniformly distributed magnetic field inside a spherical area and the desired total deviation rate along the centreline. The numerical calculations and the optimization procedure were performed on a simplified 2D axial symmetric model. The obtained results show that in the case of real conductors, the coil positions differ from the Lee-Whiting arrangement.*

Key words: *Lee-Whiting coil system, optimisation, uniform magnetic field*

1. INTRODUCTION

In many scientific investigations, it is very often necessary to place objects in a uniformly distributed magnetic field [1]. The application field is very wide including the area of biological medicine [2]-[4], magnetic resonance imaging [5],[6], cell damage recovery [7],[8] and many other fields, such as magnetometer calibration [9],[10] magnetic navigation [11], probe and sensor calibration [12], low-frequency magnetic field immunity testing [13], aerospace [14] wireless charging [15] and power transmission [16],[17].

Received November 29, 2023; revised May 23, 2024; accepted June 10, 2024
Corresponding author: Karolina Kasaš-Lažetić
University of Novi Sad, Faculty of Technical Sciences
E-mail: kkasas@uns.ac.rs
*An earlier version of this paper was presented at the 16th International Conference on applied Electromagnetics (IIEC 2023), August 28-30, 2023, in Niš, Serbia [1]

The homogeneity of the internal field can be achieved by using different coil systems of conducting wires together with the current source, which should have the role of a high-precision electromagnetic exposure system [4]. The exposure systems are usually based on coaxial coil systems to generate a linearly polarized magnetic field of high uniformity in specific volume. Very often, the coils are placed in an enclosure made of high conductivity or/and high permeability material for shielding the background magnetic field. This enclosure significantly affects the uniformity of the primarily generated magnetic field, decreasing the ability of the coil to generate a large volume of uniformly distributed magnetic field [18],[19]. To achieve a desired zone of homogeneity, attention should be paid to many elements of the system construction itself. The most frequently applied common schemes for generating these fields are Helmholtz and Merritt coils, but saddle coils, solenoid, spherical and elliptical coils are widely used, too [20].

Many investigations have been made to improve coil systems and produce larger volumes of space with uniform magnetic fields [21]. In the classic Helmholtz coil system (either square or circular), two identical magnetic coils are placed symmetrically along a common axis related to the basic plane of the experimental area. The distance between the coils is determined based on the condition that the first and second spatial derivatives of the applied field are equal to zero at the centre of the coil system. This condition is fulfilled when the distance between the circular coils d and their radii, R, or the half-length of the square coil side $a/2$ are equal ($d=R$ or $d=a/2$). Regardless of the coils' shape, the currents in both coils are the same, with the same direction of current flow [6]. To maximize the volume of homogeneity of the magnetic field, several higher derivatives can be zeroed. These conditions can be achieved using additional coils thus forming systems of three, four or five coils. The Merritt coil system with four square coils gives a larger volume of uniform magnetic field than two Helmholtz coils [3]. Sometimes the number of coils is even higher and goes up to eight.

Based on research experiments and theoretical analyses, systems with improved coaxial constructions were derived that create a larger volume of uniformly distributed magnetic field. Applying the conventional method to generate high field homogeneity in the central point of the system does not result in achieving the required homogeneity in the desired area. Accordingly, some additional information is needed, in the form of parameters such as the length of the coil centreline part or the volume of the zone with a certain value of the magnetic field. In general, the square coil systems are easier to construct, install and apply in cases when larger volumes of uniform magnetic field spaces are needed, whereas in the systems with a smaller required volume, circular coil systems are suggested [22]. Four-coil structures appear in different configurations which are suitable for optimizing their performance [23]. One of the well-known four circular coil systems is the Lee-Whiting one, providing up to 8-order field uniformity [4]. In theoretical formulas, the coils are modelled as line sources without a cross-section. In practical applications, especially when high-intensity magnetic fields are required, the cross-section of the coils cannot be neglected. It is necessary to examine the influence of the conductor's cross-section on the homogeneity of the zone of interest.

In this paper, we have compared the zone of uniformity obtained for the ideal and the real Lee-Whiting four-coil systems. Our results show that by optimizing the configuration parameters, a constant magnetic field can be achieved in arbitrary parts of the space, fulfilling the desired total deviation rate.

2. MODEL

The Lee-Whiting four-coil system consists of two circular pairs of coils with currents I_1 and I_2 of equal radii $a_1 = a_2 = a$ that are placed symmetrically $\pm z_1$ and $\pm z_2$ along a common axis with respect to the origin 0, as shown in Fig. 1. The geometry of the structure suggested the application of cylindrical coordinate system, as it is shown in Fig. 1. The Lee-Whiting coil system carries direct current in the same direction, with the current ratio of $I_1/I_2 = 2.2604$, generating a static magnetic field. Outer coils are separated by 1.8816 times their radii ($2z_1 \approx 1.8816a$), while the inner coils are separated by 0.4864 times their radii ($2z_2 \approx 0.4864a$) [4].

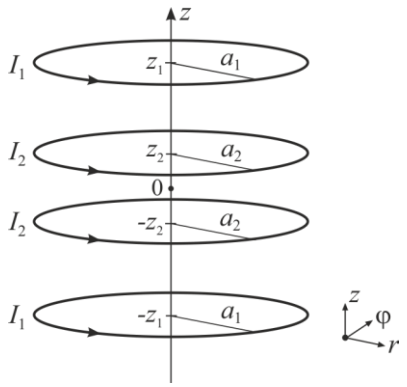

Fig. 1 Configuration of the Lee-Whiting 4-coil system

The most important parameters of the analysed Lee-Whiting 4-coil system, such as the coils radii and their positions, as well as the coils currents are shown in Table 1.

Table 1 Key parameters of the Lee-Whiting coil system

Parameter	Value
Radii of the coils (a)	0.23 m
Position of outer coils ($\pm z_1$)	±0.2164 m
Position of inner coils ($\pm z_2$)	±0.0559 m
Current of two outer coils (I_1)	1.4 A
Current of two inner coils (I_2)	0.62 A

3. CALCULATION OF MAGNETIC FLUX DENSITY

3.1. Analytical calculation

The magnetic flux density vector, $\boldsymbol{B}$, for a simple planar, filamentary circular current loop in an arbitrary point outside the conductor can be obtained analytically by applying the Biot-Savart law [24].

The problem of calculating off-axis values of the magnetic flux density vector components produced by a circular coil is somewhat more complex, due to derived formulas which are not

expressible in terms of analytic functions. It is necessary to apply complete elliptic integrals of the first and second kinds [25].

Due to the axisymmetric characteristics of circular coil structure, there can be variations of the magnetic field distribution in the radial (r) and vertical (z) direction only. For the individual current loop of the radius a, located in the $z = 0$ plane of the cylindrical coordinate system, centred at the origin and carrying current I in the positive direction, the field components, are

$$B_r = \frac{C\,z}{2\alpha^2\beta\,r}[(a^2 + r^2 + z^2)\,E(k^2) - \alpha^2 K(k^2)], \tag{1}$$

$$B_z = \frac{C}{2\alpha^2\beta}[(a^2 - r^2 - z^2)\,E(k^2) + \alpha^2 K(k^2)], \tag{2}$$

where K and E are the complete elliptic integrals of the first and second kinds, respectively, which have been illustrated in most textbooks and the literature [26]. In the above expressions, the following substitutions are applied for simplicity: $\alpha^2 = a^2 + r^2 + z^2 - 2ar$, $\beta^2 = a^2 + r^2 + z^2 + 2ar$, $k^2 = 1 - \alpha^2/\beta^2$ and $C = \mu_0 I/\pi$.

The resulting field of more than one, coaxially placed coil is equal to the vector sum of the fields generated by each coil

$$\boldsymbol{B}(r,\theta,z) = \sum_{i=1}^{n} \boldsymbol{B}_{(r,\theta,z),i}\ . \tag{3}$$

In this paper, eq. (1)-(3) were implemented in the Matlab software package for analytical calculation of the magnetic flux density distribution of the Lee-Whiting 4-coil system.

3.2. Numerical calculation

The finite element method (FEM) as a variational calculus-based numerical procedure for solving partial differential equations is suitable for handling complex geometries related to practical problems such as the one discussed in this paper. The FEM simulation in the present study was performed by applying the COMSOL Multiphysics program package. Within it, the AC/DC module's 2D-axisymmetric submodule and the Magnetic Field interface - Stationary simulation option was applied. To optimise the coil parameters to achieve a uniform B field in the desired part of space, the Optimisation module was added to the simulation process.

The FEM calculation is based on the governing differential equation for the magnetic vector potential, $\boldsymbol{A}$,

$$\Delta\boldsymbol{A} = -\mu_o \boldsymbol{J}\ , \tag{4}$$

where $\boldsymbol{J}$ denotes the imposed current density and μ_0 is the vacuum permeability [27]. The expressions for all three spatial components from the circular loop can be derived by first calculating the magnetic vector potential, $\boldsymbol{A}$. Then, the components of the vector $\boldsymbol{B}$ can be determined as

$$\boldsymbol{B} = \nabla \times \boldsymbol{A}. \tag{5}$$

To get a full description of the analysed problem, the magnetic insulation and the perfect magnetic conductor boundary condition must be additionally specified.

3.3 Model of the ideal and real coils

In this study, the ideal Lee-Whiting coil system is modelled with four volumeless circular current loops, while the real coils system is modelled with four circular current loops of rectangular cross-section.

In the case of the ideal coil system, in the analytical calculation, the total magnetic flux density is obtained by (3), as the sum of four individual filamentary circular current loops ($n = 4$). In the case of the real coil system, each of the four circular coils is portioned in N current loops passing through the nodes of a uniform rectangular grid, resulting in the total magnetic flux density as the sum of $4N$ individual filamentary circular current loops. The value of the parameter N presents a compromise between the complexity and accuracy of the model. In the analysed model, each filamentary circular current loop carries the same part of the coil current, I_1/N for the outer and I_2/N for the inner pair of the Lee-Whiting coils.

In finite element analysis (FEM), periodic conditions can greatly reduce the analysed model size. Due to axial symmetry of the Lee-Whiting coil system, as well as the knowledge about the invariant magnetic field distribution around the axis of symmetry, its 3D geometry model can be reduced and the whole calculation can be carried out solving a 2D problem in rz plane. This characteristic of the system allowed the circular current loop to be modelled with its cross-sectional geometry in the positive rz plane, only. Additionally, the analysed model is geometrically identical on either side of the plane $z = 0$, which represents the mirror symmetry plane for the coil currents, too. Applying the plane (mirror) symmetry, the number of coils could be halved.

The aforementioned advantages of the system can be effectively exploited by incorporating them into the computational process and applying appropriate boundary conditions [28].

Reducing the original geometry significantly decreased the computational complexity of the model. The simplified 2D, axisymmetric and plane symmetric models of the ideal and the real Lee-Whiting coil models for FEM calculations are presented in Fig. 2a and Fig. 2b, respectively.

The currents I_1 and I_2 in the ideal coils are modelled as point sources flowing out of rz plane in the analysed 2D axisymmetric and plane symmetric models. The real coils are presented as homogenized multi-turn conductors with N turns of copper wires inside a rectangle of dimensions $w \times h$. The homogenized multi-turn option implements a homogenized model of a coil consisting of numerous tightly wound conducting wires, separated by an electrical insulator, without the need to model each wire individually. The homogenized multi-turn feature in the COMSOL program package uses an

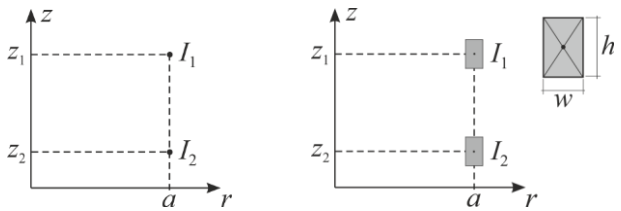

a) b)

Fig. 2 The simplified a) ideal and b) real coil 2D model for FEM calculations

appropriate equivalent geometry to model the coils. The position of the point source modelling the ideal coil coincides with the intersection of the rectangle's diagonals modelling the real coil, as it is shown in Figure 2b.

3.4. The uniformity

At an arbitrary point within the system of the loops, the magnetic field uniformity, $u(r, z)$, is defined as a deviation of the magnetic flux density at an arbitrary point, B_z, from the magnetic flux density at the centre of the system, $B_{0,}$

$$u(r,z) = \frac{\left|B_z(r,z) - B_0\right|}{B_0}. \tag{6}$$

In the applied coordinate system $B_0 = B_z(0,0)$. The uniformity is expressed in percentage per million (ppm) to find the area of high uniformity as in [28], where the deviation is less than 100 ppm.

4. OPTIMISATION ALGORITHM

In electromagnetic coil design, a desired *B*-field distribution can be achieved by changing one or more coil parameters. In the general case, the magnetic flux density distribution along a part of the centreline (on the axis of system symmetry) is not constant. The magnetic field within a desired area can be adjusted by applying certain optimization techniques, i.e., by changing the driving currents of the coil, the vertical position of the turns, their radii, or the combination of these parameters.

The optimization problem can be formally stated by applying the appropriate objective function. To achieve the desired magnetic field distribution, in this paper the objective function is expressed as

$$\frac{1}{z_{\text{opt}}} \int_0^{z_{\text{opt}}} \frac{\left|B_z(0,z) - B_0\right|}{B_0} \, \mathrm{d}z, \tag{7}$$

which minimizes the relative deviation between the *z*-component of the magnetic flux density vector, B_z, and the value of $B_0 = B_z(0,0)$, averaged over the coil's centreline between the points placed at $z = 0$ and $z = z_{\text{opt}}$. The defined optimisation zone $z \in \{0, z_{\text{opt}}\}$, ensures the highest uniformity on the symmetry axes, with a slight degradation in the radial direction. The objective is normalized with respect to z_{opt}, and B_0 [29]-[31].

The optimisation procedure is performed in the COMSOL Multiphysics software package, where several different optimisation algorithms are implemented. Since the underlying problem is stationary, the objective function (7) is analytically differentiable with respect to the control variables. Accordingly, the SNOPT (Sparse Nonlinear OPTimizer) procedure is chosen from the offered gradient based optimization methods. This optimisation procedure is a non-stochastic optimisation algorithm, which takes advantage of the analytically computed gradients of both the objective function and all the constraints. In the optimization process, the optimality tolerance is set to 10^{-6}. Compared to other optimization procedures included in COMSOL, the SNOPT requires relatively few evaluations of the problem functions [32].

The optimization procedure is performed for the real coils with rectangular cross section for several different dimensions, preserving the same current ratio and radii as those listed in Table 1. The radii given in Table 1 correspond to the position of the point source, modelling the ideal coil which is located at the middle point of the real rectangular coil model, as is shown in Fig. 2b and mentioned in Section 3.3. The target goal is to find the vertical positions of each coil (the distance between inner/outer coils) that ensure the same or nearly the same uniformity as the one theoretically obtained in [33].

5. RESULTS

The distribution of the magnetic flux density vector for the ideal Lee-Whiting 4-coil system and the determined uniformity zones of 100 ppm and 1000 ppm are presented in Fig. 3. The calculations are performed both analytically applying the MATLAB platform, and numerically in the COMSOL program package as is described in Section 3.

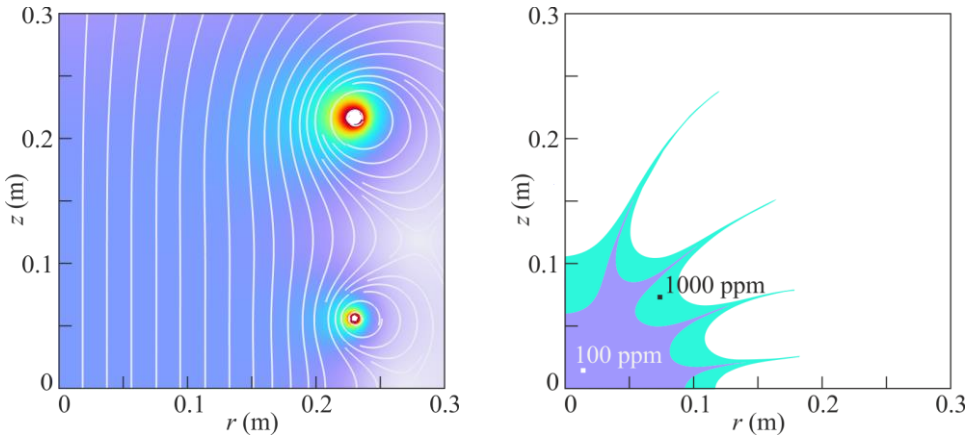

Fig. 3 a) Magnetic flux density distribution and b) the uniformity of the ideal Lee-Whiting 4-coil system

Both calculation types give the same results of the magnetic flux density vector distribution and the area of 100 ppm uniformity as in [34], proving that both models are well designed for the further analysis of the real coils.

The magnetic flux density vector distribution uniformity, $u(r, z)$, for the ideal and the real Lee-Whiting four-coil system, calculated in the COMSOL program package and the MATLAB package are presented in Fig. 4 and Fig. 5, respectively. In the first analysed case, in the real system, all coils have the same cross-section of 10×20 mm^2, with $h = 20$ mm, while in the second case, the cross-section is set to be 20×40 mm^2, with $h = 40$ mm. The shapes of uniformity presented in Fig. 4 and Fig. 5 indicate high agreement of the results obtained applying these two methods, yet the analytical calculations are much faster and with less memory consumption than the numerical, FEM based calculations.

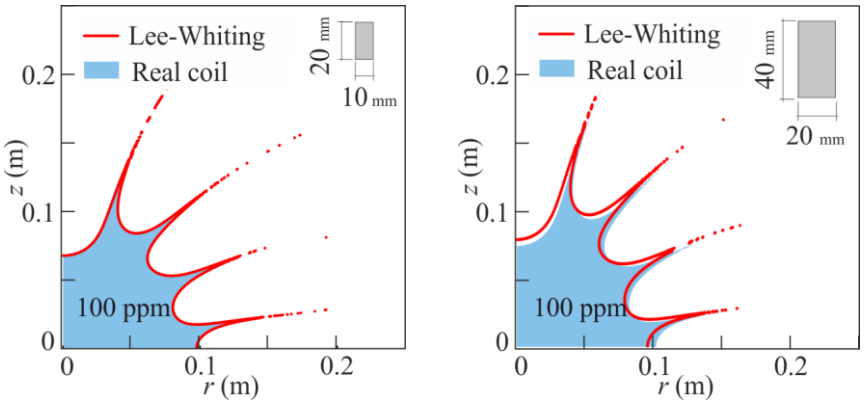

Fig. 4 FEM based uniformity calculations for the ideal Lee-Whiting 4-coil system and real coils at the same positions with cross-section: a) 10×20 mm^2, b) 20×40 mm^2

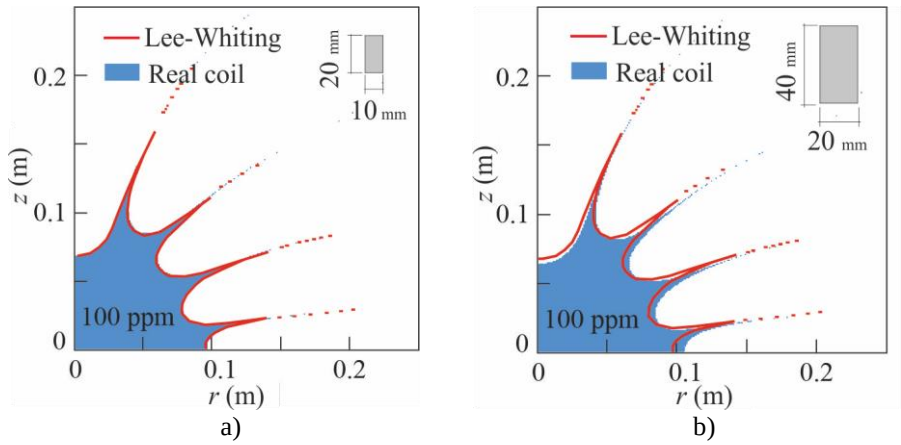

Fig. 5 Analytically based uniformity calculations for the ideal Lee-Whiting 4-coil system and the real coils at the same positions with cross-section: a) 10×20 mm^2, b) 20×40 mm^2

To examine the influence of the cross-section area of a real conductor on the magnetic flux density distribution, compared to the ideal case, the entire calculation was repeated for a rectangular cross-section of doubled dimensions, 20×40 mm^2. The uniformity zone of 100 ppm is slightly lower in the case of a real coil of doubled cross-section area than for the idealized coil system, as is shown in Fig. 4b. The obtained results indicated the need to find the new positions for the real coils with a cross section of 20×40 mm^2 to increase the zone of defined uniformity. The calculations also show that using the initial positions of the Lee-Whiting coils given in Table 1, the zone of uniformity decreases as the coil cross-section increases.

Starting from the initial positions of the ideal coils, listed in Table 1, the new positions of the real rectangular coil model were determined applying the optimization algorithm described in Section 4. The values z_1 and z_2 in Table 2 represent the optimized positions of the real coil's centre-points. The variable r_o represents the radius of the spherical area within the desired uniformity value has been reached.

Table 2 The optimized *z*-positions of the real coil's centre-points

Cross-section w (mm) × h (mm)	z_1 (mm)	z_2 (mm)	r_o(mm) 100 ppm	r_o (mm) 200 ppm
1×1	219.49	56.263	93.5	>100
2×2	219.51	56.277	94.9	>100
2×4	219.87	56.287	94.5	>100
4×8	219.96	56.301	95.6	>100
8×16	217.96	56.125	84.4	92.6
10×20	217.56	56.025	78.0	88.2

The trial-and-error method starts by setting the lowest convergence error to the obtained optimized positions in the acceptable time frame. The number of iterations, for the first three cross sections listed in Table 2 are 15, 27 and 25, respectively, with the convergence error of $1e^{-5}$. The calculation time was 154 s, 181 s and 220 s, respectively. It can be concluded that increasing the size of the cross-section, also increases the number and the time of iterations. If a calculation fails, the convergence error is increased.

The number of iterations, for the next two cross sections listed in Table 2 are 9 and 10, respectively, with the convergence error of $2e^{-5}$. The calculation time was 150 s and 167 s, respectively. The biggest cross-section that the applied algorithm could solve was 10×20 mm^2, with the convergence error of $5e^{-5}$, 10 iterations in 320 seconds. All calculations are performed on 64-bit operating system with Intel® Core™ i5-4670 CPU at 3.6 GHz with 32 GB of installed RAM. In our study, adaptive meshing was applied, refining the mesh selectively near the *z* axis and around the conductors, to improve the overall quality of the mesh. Depending on the cross section the resulting mesh has between 4500 and 5000 domain elements.

Fig. 6 shows the uniformity $u(0, z)$, for the coils with parameters listed in Table 2. For all analysed coils, a zone could be found bounded with r_o where the uniformity is below 100 ppm. The uniformity of 200 ppm is obtained slightly above 100 mm for all coil sizes except the last two where it is achieved slightly below 100 mm. In Fig. 7 the uniformity of the same coils, listed in Table 2 is shown but without the optimization algorithm. Instead, the original Lee-Whiting positions of the coils are applied. It could be noticed that the uniformity is nearly the same for all six coil systems, and it resembles the optimized 10×20 mm^2 coil cross-section. The overall conclusion is that in the case of a real coil some new positions of the coils could be found to achieve higher uniformity.

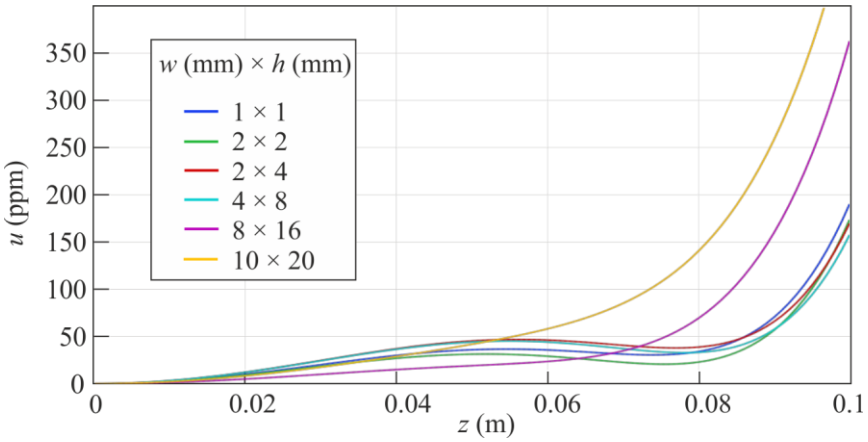

Fig. 6 Uniformity of coil cross-sections listed in Table 2 on the axis of symmetry optimized to achieve target uniformity up to z_{opt} = 10cm

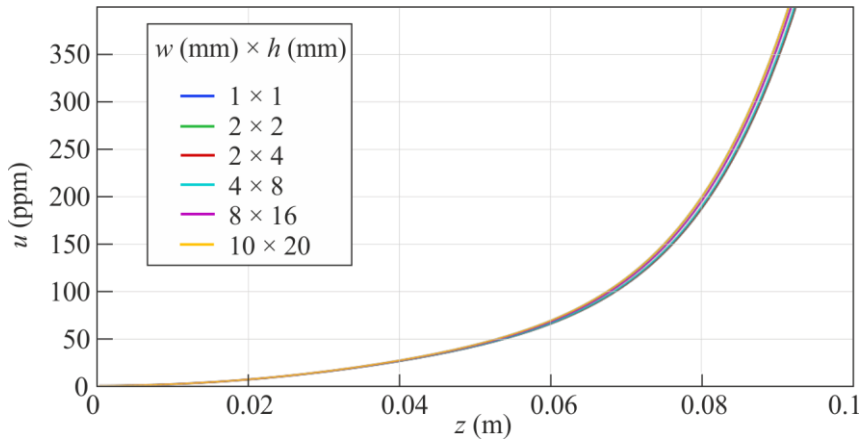

Fig. 7 Uniformity of coils with cross-sections listed in Table 2 on the axis of symmetry using the Lee-Whiting coil positions

To evaluate the effective uniform area space size, the maximum normalised space radius, R_{max} is usually applied as a parameter. It is calculated as the ratio of the maximum radius with defined uniformity, r, and the inner coil radius a, for the given coil. For example, the uniformity of 100 ppm of the ideal Lee-Whiting coil is inside a spherical zone with the maximum radius r = 0.066 m, so $R_{max} = r/a$ = 0.287. Increasing the target uniformity results in the increase of the radius of the spherical zone [23].

Fig. 8a shows the zones with uniformity of 100 ppm and 1000 ppm obtained for the ideal Lee-Whiting 4-coil system and the real coil system with cross section 10 × 20 mm^2 for which a new vertical position is obtained according to the optimisation algorithm.

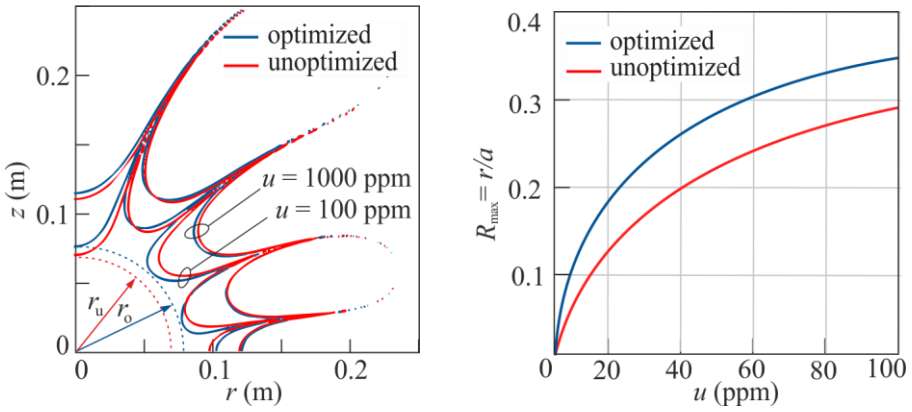

a) b)

Fig. 8 a) Uniformity and b) maximum normalised space radius for the Lee-Whiting 4-coil system with cross-section 10×20 mm^2 using z_1 and z_2 listed in Table 1 and Table 2

Comparing the uniformity for the ideal and real coil's system it could be seen that applying the optimisation algorithm the uniformity of the real coil system is improved. In Fig. 8b the maximum normalised space radius for these two coils systems is compared.

Comparing the radius $R_{max} = 0.287$ for the original Lee-Whiting coil, for $u = 100$ ppm, and the radius $R_{max} = 0.337$ for the real coil after optimization, an improvement of about 16% is achieved. Increasing the observed value of uniformity, the improvement decreases. In particular, for $u = 1000$ ppm an improvement about 4% is reached.

6. Conclusion

Uniformly distributed magnetic fields are widely used in many different applications. Circular coils provide homogeneity in a smaller area than the square ones but are easier to produce. In this paper, we tried to answer the question to what extent the real cross-section of the coil affects the magnetic field distribution, compared to the field distribution generated by the current flowing in the ideal conductor.

It is shown that both the developed analytical procedure in MATLAB and the generated numerical model in COMSOL give very similar results for the magnetic flux density vector distribution and its uniformity. Calculating the magnetic flux density vector distribution uniformity for the real and the ideal Lee-Whiting four-coil system considering two different cross-sections of the real conductor, it can be concluded that the bigger cross section slightly degraded the uniformity zone.

The results of the study demonstrated that in the coil parameters optimisation process, to reach the desired zone of uniformity, the influence of the real coil cross-section cannot be neglected. In the case of a real coil, some new positions of the coils were found to achieve higher uniformity. According to the optimisation results, the uniformity of the real coil's system is improved.

Acknowledgment: *This paper is supported by the Provincial Secretariat for Higher Education and Scientific Research of the Autonomous Province of Vojvodina, through the project, no: 142-451-3190/2023-01/01.*

REFERENCES

[1] K. Kasaš-Lažetić, M. Milutinov, T. Spasić and G. Mijatović, "Improving the Coil Design Parameters to Achieve a High Uniformity Magnetic Field", In Proceedings of the 16th International Conference on Applied Electromagnetics (ПЕС 2023) Conference, 2023, pp. 85–88.

[2] J. L. Ristić-Djurović, S. Gajić, A. Ilić, N. Romčević et al., "Design and Optimization of Electromagnets for Biomedical Experiments with Static Magnetic and ELF Electromagnetic Fields", *IEEE Trans. Ind. Electron.*, vol. 65, no. 6, pp. 4991–5000, Nov. 2017.

[3] D. Herceg, A. Juhas and M. Milutinov, "A Design of a Four-square Coil System for Biomagnetic Experiment", *Facta Universitas, Series: Electronics and Energetics*, vol. 22, no. 3, pp. 285–292, Dec. 2009.

[4] J. L. Kirschvink, "Uniform Magnetic Fields and Double-wrapped Coil Systems: Improved Techniques for the Design of Bioelectromagnetic Experiments", *Bioelectromagnetic*, vol. 13, no. 5, pp. 401–411, May 1992.

[5] S. Ghaly, K. Alsnaie and A. Ali, "Design and Modeling of a Radiofrequency Coil Derived from a Helmholtz Structure", *Eng. Technol. Appl. Sci. Res.*, vol. 9, no. 2, pp. 4037–4040, April 2019.

[6] S. Ghaly and M. Khan, "Design, Simulation, Modeling and Implementation of a Square Helmholtz Coil in Contrast with a Circular Coil for MRI Application", *Eng. Technol. Appl. Sci. Res.*, vol. 9, no. 6, pp. 4990–4995, Dec. 2019.

[7] C. Cezar, E. Roche, H. Vandenburgh, at al., "Biologic-free Mechanically Induced Muscle Regeneration", *Proc. Natl. Acad. Sci. U.S.A*, vol. 113, no. 6, pp. 1534–1539, Feb. 2016.

[8] Y. Zhao, T. Fan, J. Chen et al., "Magnetic Bioinspired Micro/Nanostructured Composite Scaffold for Bone Regeneration", *Colloids Surf. B: Biointerfaces*, vol. 174, pp. 70–79, Feb. 2019.

[9] D. Yang, Z. You, B. Li et al., "Complete Tri-Axis Magnetometer Calibration with a Gyro Auxiliary", *Sensors*, vol. 17, no. 6, pp. 1–21, May 2017.

[10] C. Qian, L. Ying, T. Junjian, Zh. Tian, H. Xing and Zh. Yueyang, "In Situ Calibration of Coils Constant in a Spin-exchange Relaxation-free (SERF) Co-magnetometer", *Measurement*, vol. 214, pp. 1–9, June 2023.

[11] S. Kim and K. Ishiyama, "Magnetic Robot and Manipulation for Active-locomotion with Targeted Drug Release", *IEEE/ASME Trans. Mechatron.*, vol. 19, no. 5, pp. 1651–1659, Oct. 2014.

[12] A. Zikmund and P. Ripka, "Calibration of the 3D Coil System's Orthogonality", *IEEE Trans. Magn.*, vol. 49, no. 1, pp. 66–68, Jan. 2013.

[13] Y. Yang, Y. Song, L. Jiang et al., "An Improved Two-Coil Configuration for Low-Frequency Magnetic Field Immunity Test and its Field Inhomogeneity Analysis", *IEEE Trans. Ind. Electron.*, vol. 65, no. 10, pp. 8204–8214, Oct. 2018.

[14] D. Batista, F. Granziera, M. Tosin and L. de Melo, "Three-Axial Helmholtz Coil Design and Validation for Aerospace Applications", *IEEE Trans. Aerosp. Electron. Syst*., vol. 54, no. 1, pp. 392–403, Oct. 2017.

[15] K. Kamalapathi, P. S. Rao Nayak and V.K Tyagi, "Development and Analysis of Three-coil Wireless Charging System for Electric Vehicles", *Int. J. Circ. Theor. Appl*., vol. 50, no. 1, pp. 249–271, Oct. 2021.

[16] D. Vinko, D. Bilandžija and V. Mandarić Radivojević, "Optimization of a Two-layer 3D Coil Structure with Uniform Magnetic Field", *Hindawi, Wireless Power Transfer*, 2021, pp. 1–11, Oct. 2021.

[17] D. Bilandžija, D. Vinko and I. Bionić, "Achieving Uniform Magnetic Field with Rectangular Coil in Wireless Power Transmission System", In Proceedings of the 61st International Symposium ELMAR, 2019, pp. 1–4.

[18] A. Juhas, N. Pekarić-Nađ and H. Toepfer, "Magnetic Field of Rectangular Current Loop with Sides Parallel and Perpendicular to the Surface of High-permeability Material", *Serbian Journal of Electrical Engineering*, vol. 11, no. 4, pp. 701–717, Dec. 2014.

[19] Q. Cao, D. Pan, J. Li, Y. Jin, Z. Sun, S. Lin, G. Yang and L. Li, "Optimization of a Coil System for Generating Uniform Magnetic Field Inside a Cubic Magnetic Shield", *Energies*, vol. 11, pp. 1–14, March 2018.

[20] Z. Xuehua, L. Chuangchuang, S. Hao, M. Yutong and Ch. Hongde, "Design of Improved Four-coil Structure with High Uniformity and Effective Coverage Rate", *Helion*, vol. 9, no. 4, pp. 1–18, April 2023.

[21] Y. Lu, Y. Yang, M. Zhang, R. Wang, L- Jiang and B. Quin, "Improved Square-Coil Configurations for Homogeneous Magnetic Field Generation", *IEEE Trans. Ind. Electron.*, vol. 69, no. 6, pp. 6350–6360, June 2022.

[22] R. Merritt, C. Purcell and G. Stroink, "Uniform Magnetic Field Produced by Three, Four and Five Square Coils", *Rev. Sci. Instrum.*, vol. 54, no. 7, pp. 879–882, July 1983.
[23] H. Liangliang. X. Jinzhang. Zheng Q., Z. Xun and H. Zongyuan, "A Novel Understanding of Circular Four-coil Configuration for Uniform Magnetic Field Generation", *IJEEE*, pp. 1–13, March 2021.
[24] J. Simpson, J. Lane, Christopher Immer and Robert Youngquist, "Simple Analytic Expressions for the Magnetic Field of a Circular Current Loop", *NASA/TM-2013-217919*, pp. 5–7, 2001.
[25] Ch. Yuessen, "Numerical Calculation for the Magnetic Field in Current-carrying Circular Arc Filament", *IEEE Trans. Magn.*, vol. 34, no. 2, pp. 502–504, March 1998.
[26] M. W. Garrett, "Calculation of Fields, Forces and Mutual Inductances of Current Systems by Elliptic Integrals", *J. Appl. Phys.*, vol. 34, no. 9, pp. 2567–2573, Sept. 1963.
[27] B. D. Popovic, *Electromagnetics*, Beograd: Gradjevinska knjiga, 2000.
[28] Z. Xuehua, L. Chuangchuang, S. Hao, M. Yutong and Ch. Hongde, "Design of Improved Four-coil Structure with High Uniformity and Effective Coverage Rate", *Helion*, vol. 9, no. 4, pp. 1–18, April 2023.
[29] https://www.comsol.com/blogs/exploiting-symmetry-simplify-magnetic-field-modeling/#Modeling%20A%20Coil%20with%20Three%20Symmetry%20Planes, Retrieved February 28, 2024.
[30] https://www.comsol.com/support/learning-center/article/Optimizing-a-Coil-to-Achieve-a-Desired-B-Field-9951 , Retrieved July 30, 2023.
[31] https://www.comsol.com/blogs/3-ways-to-optimize-the-current-in-electromagnetic-coils/ , Retrieved July 30, 2023.
[32] P. E. Gill, W. Murray and M. A. Saunders, "SNOPT: an SQP Algorithm for Large-scale Constrained Optimization", *SIAM Rev.*, vol. 47, no. 1, pp. 99–131, Feb. 2005.
[33] G. E. Lee-Whiting, *Uniform Magnetic Field*, Atomic Energy of Canada, Ltd. Chalk River Project Research and Development, Report CRT/673, 1957, pp. 1–31.
[34] Ch. P. Gooneratne, A. Kumasi, S. Yamada, S. C. Mukhopadhyay and J. Kosel, "Analysis of the Distribution of Magnetic Fluid inside Tumors by a Giant Magnetoresistance Probe", *PLoS ONE*, vol. 8, no. 11, e81227, pp. 1–14, 2013.